HHS Public Access

Author manuscript

Gerontology. Author manuscript; available in PMC 2017 February 26.

Published in final edited form as:

Gerontology. 2016 ; 62(5): 519–529. doi:10.1159/000443793.

Programmed cell death genes are linked to elevated creatine kinase levels in unhealthy male nonagenarians

Sangkyu Kim[1], **Eric Simon**[2], **Leann Myers**[3], **L. Lee Hamm**[2], and **S. Michal Jazwinski**[1]

[1]Tulane Center for Aging and Department of Medicine, Tulane University Health Sciences Center, New Orleans, LA 70112, USA

[2]Department of Medicine, Tulane University Health Sciences Center, New Orleans, LA 70112, USA

[3]Department of Biostatistics and Bioinformatics, School of Public Health and Tropical Medicine, Tulane University Health Sciences Center, New Orleans, LA 70112, USA

Abstract

Declining health in the oldest-old takes an energy toll for simple maintenance of body functions. The underlying mechanisms, however, differ in males and females. In females, the declines are explained by loss of muscle mass, but this is not the case in males in whom they are associated with increased levels of circulating creatine kinase. This relationship raises the possibility that muscle damage rather than muscle loss is the cause of the increased energy demands of unhealthy aging in males. We have now examined factors that contribute to the increase in creatine kinase. Much of it (60%) can be explained by a history of cardiac problems and lower kidney function, while being mitigated by moderate physical activity, reinforcing the notion that tissue damage is a likely source. In a search for genetic risk factors associated with elevated creatine kinase, the Ku70 gene *XRCC6* and the ceramide synthase gene *LASS1* were investigated because of their roles in telomere length and longevity and healthy aging, respectively. Single-nucleotide polymorphisms in these two genes were independently associated with creatine kinase levels. The *XRCC6* variant was epistatic to one of the *LASS1* variants but not to the other. These gene variants have potential regulatory activity. Ku70 is an inhibitor of the pro-apoptotic Bax, while the product of Lass1, ceramide, operates in both caspase-dependent and independent pathways of programmed cell death, providing a potential cellular mechanism for the effects of these genes on tissue damage and circulating creatine kinase.

Keywords

aging; creatine kinase; programmed cell death; kidney; heart

Address correspondence to: Sangkyu Kim, PhD, Tulane Center for Aging and Department of Medicine, Tulane University Health Sciences Center, 1430 Tulane Ave., SL-12, New Orleans, LA 70112, USA. Tel.: 504–988-3091; fax: 504-988-8835; skim5@tulane.edu.

Conflicts of interests
None declared.

Supplementary material
Supplementary material mentioned in the text are available online.

Introduction

Previously, we found that elevation of resting metabolic rate (RMR) is associated with declining health in nonagenarians [1]. RMR represents the energy used to maintain the integrity and functionality of the body. It accounts for the bulk (60%–70%) of total daily energy expenditure. As a quantitative measure of heathy aging, we used the frailty index FI_{34} composed of 34 common health and function variables [2]. FI_{34} increases exponentially with age and is heritable, which points to a genetic contribution to the age-dependent decline in health and function ability. In analyzing the association of RMR with FI_{34}, we noticed gender differences in the regression outcomes for some of the covariates: In nonagenarian males, FI_{34} was positively correlated with circulating creatine kinase (CK); in nonagenarian females, fat mass (FM) and fat-free mass (FFM) were associated with FI_{34} [1].

CK is often used as a clinical marker of muscle damage [3–5]. It catalyzes reversible conversion of creatine and ATP to phosphocreatine and ADP [6]. In cells that need a large amount of ATP, phosphocreatine serves as an energy reservoir that can rapidly provide ATP. The three major isoforms of cytoplasmic CK are CK-MM, CK-MB, and CK-BB, which are abundant in skeletal muscle, cardiac muscle, and brain, respectively. Cells also have mitochondrial CK, which exists in two forms: ubiquitous and sarcomeric [7]. Typical laboratory tests do not distinguish the types of CK. The cytoplasmic and mitochondrial CK form the phosphocreatine shuttle or circuit that can harness energy generated by mitochondrial oxidative phosphorylation and transfer it to the cytoplasm for rapid, anaerobic use [8,9]. Thus, CK is a crucial enzyme for generation of phosphocreatine that functions as an energy buffer and as an energy carrier [7].

CK in blood is used as a biomarker of various types of muscle damage, such as rhabdomyolysis (severe muscle breakdown), muscular dystrophy, and autoimmune myositis (muscle inflammation) [10,11]. Because of its abundance in cardiac muscle cells, CK is frequently associated with cardiac pathology, such as heart attack (myocardial infarction) and inflammation (myocarditis) [12]. CK elevation is also associated with acute renal failure in some cases [11,13]. A number of other factors are known to contribute to CK elevation. For example, statin use may be associated with elevation of the CK level [14–17]. In hypothyroid patients, a decrease in serum T3 is associated with a significant increase in CK [18].

The presence of cellular CK in the circulation is mostly due to leakage from damaged cells. For example, acute renal failure can follow rhabdomyolysis caused by prolonged cardiac surgery [19]. Breakdown products of damaged muscle cells (e.g., myoglobin) that are released into the bloodstream may cause kidney failure [20]. Leakage of cytosolic contents from damaged myocytes occurs in certain types of cell death. In fact, programmed cell death is a common type of cell death in myocardial infarction, ischemia/reperfusion injury, or heart failure [21–25]. Fas-mediated programmed cell death of renal tubule epithelial cells, due to loss of α(E)-catenin, is also encountered during acute injury in the aging kidney [26].

We took a genetic approach to elaborate on the male-specific association of CK with healthy aging. We chose *XRCC6* and *LASS1* (also known as *CERS1*) because we had previously

studied these genes for their roles in healthy aging and longevity. Besides, these genes are involved in apoptotic cell death. Ku70, encoded by *XRCC6*, has a dual function, non-homologous end joining of DNA ends and regulation of the pro-apoptotic Bax. A SNP at the 3' end of *XRCC6* is associated with telomere length in an allele-specific manner during aging [27]. *LASS1* is a human homolog of the budding yeast longevity assurance gene 1 (*LAG1*) [28]. *LASS1* encodes a ceramide synthase, and ceramide stimulates Fas-mediated programmed cell death [29–31]. SNPs in *LASS1*, in combination with SNPs in *HRAS1* and *APOE*, are associated with longevity and healthy aging [32]. In this article, we report our findings on the male-specific association of *XRCC6* and *LASS1* with CK.

Materials and Methods

Participants

Subjects in this study are 67 nonagenarians from the Louisiana Healthy Aging Study (LHAS) [32]. Ages of participants were based on documentary evidence and demographic questionnaires. All participants provided informed consent according to protocols approved by the respective Institutional Review Boards. The summary statistics of the variables used here are shown in table 1.

SNPs for *XRCC6* and *LASS1*

Genotyping using the Illumina GoldenGate assay was described elsewhere [32]. The *XRCC6*-linked SNP rs132793 is located about 3.6 kb downstream from the end of the last exon of *XRCC6*. This SNP is polymorphic and in Hardy-Weinberg equilibrium in both gender groups (table S1). SNPs rs2075762 and rs7252796 are located in introns of *LASS1*. They are also polymorphic and in Hardy-Weinberg equilibrium (table S1). Pairwise linkage disequilibrium (LD) blocks involving rs132793 on chromosome 22 and rs2075762 and rs7252796 on chromosome 19 were estimated using Haploview [33,34].

Data collection and management

Only Caucasian participants were included in the analyses to avoid confounding by population admixture. Origin population was inferred genetically [32]. Collection of data, calculation, and properties of FI_{34} were described in detail elsewhere [2]. Measurements of metabolic parameters used in this study were described previously [1]. Briefly, EESI is one of the three indices of the Yale physical activity survey [35]. It is calculated by multiplying the time spent on an activity by an intensity code and summing the products over all the activities for a week. FFM and FM are in proportions of total body weight, as determined by Dual-Energy X-ray Absorptiometry (DEXA). Resting Metabolic Rate (RMR) was measured by indirect calorimetry (oxygen consumption and CO_2 production) during rest (reclining position and keeping still) using a Deltatrac II metabolic cart (Sensormedics, Yorba Linda, CA), and the measurements of the last 20 minutes were averaged to calculate RMR expressed in kilocalories per 24 hours. CK levels were measured using an enzymatic assay (Beckman Coulter DXC 600 Pro System; Beckman Coulter, Fullerton, CA). The eGFR is a value from a blood test for creatinine (mg/dL), which was measured on a Beckman Coulter DXC 600 Pro using a modified rate Jaffe method [36]. It was calculated using the Chronic

Kidney Disease Epidemiology Collaboration (CKD-EPI) equation on the National Kidney Disease Education Program website [37,38].

Statistical analysis

All statistical analyses were performed using R [39]. The *lm* function in the base installation was used for multiple linear regression tests. Raw CK is not normally distributed across the entire sample. Therefore, data transformation was carried out using the *boxcox* function in the MASS library, which returned a lambda value of −0.5. Transformed CK ($CK^{-0.5}$ herein called CKt) is normally distributed (fig. S1). CK and CKt are negatively (inversely) correlated. Statistical power of multiple linear regressions was analyzed using GPower 3.1 [40].

Results

Association of CK with heart and kidney abnormalities in male nonagenarians

RMR decreases with advancing age [41]. Among nonagenarians, however, RMR was positively associated with FI_{34} (Kim et al. 2014; fig. 1). This suggests that increased energetic demands for maintenance parallel the decline in health during aging. Accompanying this RMR increase was a decrease in FFM and an increase in CK. Further analysis showed that the decrease in FFM was specific to females, while the increase in circulating CK was found only in males (Kim et al. 2014). We decided to first explore the latter relationship by examining possible factors that could contribute to circulating CK, including lower kidney function (eGFR) and heart problems (Cardiac).

CKt levels and eGFR values appeared higher in females than in males overall, but no statistical differences were detected (table 1). Among the male nonagenarians, however, those with a history of one or more heart problems appeared to show lower CKt levels compared to those without heart problems (0.097 and 0.13, respectively). Likewise, among the males, those with relatively low renal function showed lower CKt levels than those with normal renal function (0.11 and 0.14, respectively). We examined the associations of cardiac history (Cardiac) and renal function (eGFR) with CKt using two-way ANOVA and found both to be significantly associated with CKt (table 2). These associations were not observed in female nonagenarians (table S2). Because CK is inversely related to CKt, the ANOVA results indicate that higher circulating CK levels are associated with cardiac and renal abnormalities, and this association is limited to male nonagenarians.

To assess these associations more accurately, we did multiple linear regression analysis of CKt with covariate adjustments. Starting with a model including Cardiac and eGFR as two explanatory variables, we tested each of six covariates of age, FFM, RMR, IGF1, T3, and T4 as an additional explanatory variable, which were included in our previous study of energy metabolism in nonagenarians [1]. None was significant when present with Cardiac and eGFR (not shown). Various factors affect serum CK levels, including statin use and physical activity [14,42]. We tested these and found only EESI significantly enhancing the model (table 3). (We also tested body-surface area as a covariate for eGFR but found no effect.) In nonagenarian males, all three variables were significantly associated with CKt, accounting

for 60% of its total variation (p = 5.39e-6) (table 3). In contrast, none of them were significant in the female nonagenarians (not shown).

EESI is positively associated with CKt (b = 3.37e-7, p = 0.0192), which means an inverse association with CK because of the negative exponent used to obtain CKt. In other words, a unit increase in physical activity is correlated with a decrease in the circulating CK level (table 3). Similarly, eGFR is inversely associated with CK (fig. S2), while the number of heart problems is positively associated with CK. Thus, lower kidney function manifests itself in higher circulating CK levels.

Association of *XRCC6* and *LASS1* SNPs with CK

We next examined SNPs linked to *XRCC6* and *LASS1* by placing them individually in the model as additional explanatory variables. Previously, the minor allele of rs132793 was associated with longer leukocyte telomeres during aging. As shown in table 4, the additive genetic effect of the minor allele of rs132793 is positively associated with CKt (b = 0.024, p = 8.3e-5). Thus, an increase in the copy number of the minor allele is predicted to result in a decrease in the CK level, suggesting a beneficial effect. Compared with the base model in table 3, the expanded model with rs132793 did not make any marked changes in the regression outputs for EESI, eGFR, and Cardiac. However, note the large increase in the adjusted R^2 (from 0.60 to 0.78). This indicates a significant improvement in the statistical model by inclusion of the *XRCC6*-linked SNP (p = 8.4e-5).

For *LASS1*, we found rs2075762 and rs7252796 significantly associated with CKt (b = 0.026, p = 0.0061 for rs2075762; b = -0.028, p = 0.0069 for rs7252796). Neither of the *LASS1* SNPs drastically altered the regression outputs for the other explanatory variables, but both SNPs significantly increased adjusted R^2 (table 4). Interestingly, the directions of association of the *LASS1* SNPs with CKt differed: rs2075762 was positively associated with CKt (hence, inversely associated with raw CK), whereas rs7252796 was inversely associated with CKt (positively associated with CK). This indicates that these two *LASS1* SNPs have different effects on CK.

Combination of *XRCC6* and *LASS1* SNPs

Given that the three SNPs are significantly associated with CK, we were curious about combinatorial effects of these SNPs in the model (table 5). First, as with single SNPs, combinations of two or three SNPs did not drastically alter the regression outputs for EESI, eGFR, and Cardiac; they all remained significant with the same association directions as in the starting model. Second, the presence of rs132793 in *XRCC6* masked the effect of rs2075762 in *LASS1*, in the sense that when they were together the significance of rs2075762 disappeared (Model 1 and 4). A masking effect of rs132793 over rs7252796 in *LASS1* was less apparent (Model 2 and Model 4). Without the *XRCC6* SNP, the two *LASS1* SNPs were fully effective (Model 3). Therefore, the effect of the *XRCC6* SNP was epistatic to the *LASS1* SNPs. Interestingly, according to Model 3, the *LASS1* SNPs rs2075762 and rs7252796 were statistically independent.

Putative functions of the SNPs

SNP rs132793 is in high LD with three SNPs in the promoter region of *XRCC6* (fig. 2). Of these, rs132770 in the 5' promoter region of *XRCC6* has regulatory potential ($r^2 = 0.92$ with rs132793). It is located 30 nucleotides upstream of the start of the first exon and falls within a number of potential transcription factor binding sites (fig. S3). Regarding the *LASS1* SNPs, rs2075762 and rs7252796 are not in LD with each other (fig. 2).

We further explored genomic features around these SNPs available in online databases. Regarding rs132793, as shown in figure 3a, a number of regulatory elements lie on or near the locus. These include clusters of H3K4Me1 and H3K27Ac histone marks, DNase I sensitive sites, and transcription factor binding sites. All these features coincide with the presence of several strong enhancers across multiple cell lines, as shown by the Genome Segmentations from ENCODE [43]. Thus, rs132793, in addition to its high genetic correlation with SNPs in the promoter region of *XRCC6*, is likely to possess its own regulatory function. As for rs2075762 in *LASS1*, no particular functional annotations were available except that it is near a splice junction (fig. 3b). According to HaploReg [44], rs7252762 is in high LD with rs2018392 ($r^2 > 0.8$). As shown in figure 3b, rs2018392 overlaps a DNase I hypersensitive site and a number of potential transcription factor binding motifs, such as binding sites for SP1, SP4, IRF1, etc. Thus, based on its linkage with rs2018392, rs7252796 may have a regulatory influence on *LASS1*.

Discussion

Many factors can lead to CK elevation in the serum. These include endocrine disorders (hypothyroidism), statins (HMG-CoA reductase inhibitors), strenuous exercise, muscle trauma, surgery, cardiac diseases, and acute kidney diseases [11]. Cardiovascular diseases are leading contributors to mortality and morbidity, and much is known about the CK elevation associated with cardiac pathology [12]. CK elevation is also associated with renal failure. We found positive associations of cardiac and renal abnormalities with CK in male nonagenarians only. These associations were apparent with adjustment for the differences in age, FFM, RMR, statin use, thyroid hormones, and physical activity.

In our study, physical activity, represented by EESI, is inversely associated with CK in male nonagenarians (table 3). However, strenuous physical activity, including exercise, is known to increase CK levels. Our study sample is comprised of nonagenarians, and EESI summarizes light or moderate physical activity that does not require vigorous muscular performance. Thus, EESI likely reflects the health status of the oldest-old, and higher EESI (healthier status) is associated with lower CK in our sample. We found no differences in eGFR (kidney function) between men and women (table 1). Some studies have identified differences between the genders, while others have not. Our study examines eGFR in light of other health variables in the oldest-old for whom such information has been lacking.

Because elevated levels of circulating CK result from leakage of cellular contents from cells that undergo damage and death, we investigated two genes, *XRCC6* and *LASS1*, that are known to be involved in programmed cell death as well as in aging and longevity. Ku70, encoded by *XRCC6*, is involved in non-homologous end joining, a mechanism of telomere

maintenance [45–48]. Previously, we associated *XRCC6* rs132793 with telomere length; the minor allele was associated with longer telomeres [27]. In the current study, the minor allele was also associated with lower CK levels, expanding the beneficial effect of the minor allele. Another function of Ku70 is to regulate the pro-apoptotic protein Bax. Normally, Ku70 complexes with Bax, preventing it from functioning. However, downregulation or modification of Ku70 results in Bax-dependent programmed cell death of neuroblastoma cells [49]. On the other hand, Ku70 overexpression suppresses Bax-mediated programmed cell death [50]. Furthermore, Bax-dependent cell death can be induced by overexpression of an acetyltransferase, by ablation of a histone deacetylase (HDAC), or by an HDAC inhibitor, such as Trichostatin A [51,52]. These results indicate that acetylation of Ku70 blocks Ku70-Bax complex formation, resulting in release of free Bax into mitochondria. Thus, one scenario would be that Ku70 production is suppressed or the protein is more acetylated in damaged cells, which triggers Bax-dependent programmed cell death resulting in the release of cell contents into the extracellular fluid.

No experimental data are available for the effect of rs132793 on Ku70 expression in vivo. However, computational merging of chromatin-immunoprecipitation sequencing data across multiple cell lines indicates that this variant is located in a regulatory region of the genome (figure 3a). Based on the associated traits and assuming a direct effect of the SNP on gene expression, we predict that the minor allele of rs132793 will increase Ku70 expression, resulting in better genome maintenance (longer telomeres) and higher cell survival (fewer cell death events).

Senescent fibroblasts have total cellular levels of Ku70 several-fold lower than young fibroblasts [53], implying an age-dependent decrease in Ku70. Interestingly, these fibroblasts also differ in subcellular levels of the Ku proteins: young fibroblasts have almost equal levels of Ku proteins between the cytoplasmic and nuclear fractions; however, senescent fibroblasts have dramatically reduced levels of cytoplasmic Ku proteins while maintaining the nuclear Ku levels unchanged. Thus, these results imply increased susceptibility of aging cells to Bax-dependent cell death (by failure to block Bax in the cytosol) while maintaining the NHEJ repair function in the nucleus. This sparing of NHEJ may partially mitigate the decline in Ku70 expression with age and help maintain telomere length while delaying senescence in aging cells.

LASS1 is also involved in programmed cell death through the action of its product ceramide. In cultured rat skeletal muscle myotubes, ceramide accumulation is associated with programmed cell death [54]. Furthermore, C(2)-ceramide stimulates programmed cell death in myotubes, whereas fumonisin B(1), a ceramide synthase inhibitor, suppresses apoptotic events induced by palmitate. Palmitate is one of the precursors for de novo ceramide synthesis. Similarly, in human vascular smooth muscle cells, ceramide synthesis increases following nitric oxide (NO)-induced programmed cell death, and treatment of the cells with C(2)-ceramide induces programmed cell death [55]. Ceramide enhances Bax-induced apoptotic events [56]. The effect of ceramide is not straightforward because ceramide-induced mitochondrial activation in *BAX*-transfected cells is caspase-independent, whereas apoptotic events downstream of mitochondrial activation, such as DNA fragmentation, are caspase-dependent. Gemcitabine and Doxorubicin, which are used in cancer chemotherapy,

are capable of inducing *LASS1* expression, and the resulting C(18)-ceramide generation results in the induction of caspase-3 activation [57]. Thus, overexpression of *LASS1* enhances the growth-inhibitory effects of the drugs on human head and neck squamous cell carcinomas.

The two *LASS1* variants, rs2075762 and rs7252796, had different effects: the minor allele of the former was associated with lower CK level, while the minor allele of the latter had the opposite effect (table 4). Computational merging of chromatin-immunoprecipitation sequencing data across multiple cell lines indicates that these variants are located in a regulatory regions of the genome (figure 3b). However, no experimental data are available for the effects of these SNPs on ceramide synthesis. Assuming that these SNPs are within *LASS1* regulatory sequences, the minor allele of rs2075762 is likely to have a negative effect on *LASS1* expression, whereas the minor allele of rs725796 is likely to have a positive effect, reducing or increasing production of ceramide synthase and hence ceramide, respectively. Because the two SNPs were statistically independent (table 5), they are likely to affect different regulatory sequences, supporting this interpretation.

Various apoptotic indicators are associated with aging muscles. A significant increase in DNA fragmentation is associated with an increase in apoptosis-inducing factor AIF in thigh muscles of aging humans [58]. The aging thigh muscles also showed increased expression of Bax. Compared with muscles from young men (mean age = 24 years), muscle cells from older men (mean age = 71 years) showed higher mitochondrial permeability transition pore sensitization and a several-fold higher proportion of endonuclease G-positive nuclei [59]. A similar apoptotic tendency is also seen in adult stem cells. Satellite cells, which are myogenic stem cells important for skeletal muscle regeneration, from old subjects (mean age = 71 years) are more prone to apoptotic cell death, compared with those from young subjects (mean age = 27 years) [60]. The cell death genes upregulated in the satellite cells from old subjects include the caspase 9 gene, whose activation is promoted by cytochrome c [61]. In a study of a cohort of elderly people of ages ≥ 70, levels of caspase-8, cleaved caspase-3, cytosolic cytochrome c, and mitochondrial Bak are significantly correlated with a thigh volume measure, and levels of cleaved caspase-3 and mitochondrial Bax and Bak are significantly correlated with a gait speed measure [62]. All these results indicate that aging muscles seem to be more prone to various cascades of apoptotic cell death. Currently, the underlying mechanism for the male-specific CK associations is largely speculative. Numerous gender differences are found in various biological and clinical settings, and this includes geriatric settings [63]. For example, women tend to show reduced inflammatory responses compared to men following eccentric exercise, even though similar muscle damage is found in each [64]. Some ascribe the sex differences in muscle damage to the female sex hormone 17β-estradiol. However, the role of the female sex hormone in nonagenarian females is questionable. Because extracellular CK is due to leakage largely from muscle cells, the level of circulating CK will be affected by muscle mass and composition. Men have higher FFM than women, which agrees with the higher CK level of men compared to women in the same age group, as shown in table 1. The idea of muscle mass as the main source for the variation in the CK level is further supported by the observation that the frequencies of male and female nonagenarians with low renal function or heart problems are not different (table 1). However, it is possible that given the same

incidence of morbidity, the mass of damaged muscle cells or the extent and severity of the damage might be higher in men than in women, leading to a higher CK elevation in men. Our sample of nonagenarian men and women displayed similar physical activity levels, while the men had a substantially higher muscle mass (table 1). However, physical activity is associated with lower CK levels and only in men. This juxtaposition further highlights the differences between the genders in their patterns of heathy aging.

Our previous and current findings point to the importance of tailoring diagnostic and therapeutic interventions in the elderly based on their gender. We have expanded on the need for this approach by examining genetic determinants underlying the increase in CK levels in men that are associated with decline in healthy aging. Certain variants of *XRCC6* and *LASS1* are risk factors for increases in circulating CK. Thus, these SNPs (and others in these genes) are candidates for a precision medicine approach to healthy aging. In this fashion, precision medicine would be applied not only to therapeutic but also to preventive strategies [65].

Although our analysis begins with a larger sample, we hone in on a subsample of nonagenarian males in the search for genetic risk factors, which warrants caution in drawing conclusions. According to power analysis based on unadjusted R^2 and the numbers of predictors specified in individual models, the 1-β values of all the models described here exceed 0.9 at n = 30 and α = 0.05. We are aware, however, that such post-hoc power analysis can be misleading, especially when applied to nonsignificant statistical models [66,67]. With this caveat, we found that morbid cardiac history and low renal function are associated with elevated levels of serum CK in nonagenarian males only. We linked two genes involved in programmed cell death, *XRCC6* and *LASS1* with CK levels. The relevant SNPs in these genes are in non-coding regions, but functional annotations indicate that they are likely to have a regulatory role.

Supplementary Material

Refer to Web version on PubMed Central for supplementary material.

Acknowledgments

We thank the people of Louisiana for participation in our studies. We also thank Jennifer Rood at Pennington Biomedical Research Center, Baton Rouge, LA, USA, for providing lab variables. This study was supported by grants from the National Institute on Aging of the National Institutes of Health (P01AG022064 to S.M.J.), the National Institute of General Medical Sciences of the National Institutes of Health (P20GM103629) to S.M.J. and S.K., the Louisiana Board of Regents through the Millennium Trust Health Excellence Fund [HEF(2001–06)-02] to S.M.J, and by the Louisiana Board of Regents RC/EEP Fund through the Tulane-LSU CTRC at LSU Interim University Hospital.

References

1. Kim S, Welsh DA, Ravussin E, Welsch MA, Cherry KE, Myers L, Jazwinski SM. An elevation of resting metabolic rate with declining health in nonagenarians may be associated with decreased muscle mass and function in women and men, respectively. J Gerontol A Biol Sci Med Sci. 2014; 69:650–656. [PubMed: 24162336]
2. Kim S, Welsh DA, Cherry KE, Myers L, Jazwinski SM. Association of healthy aging with parental longevity. Age (Dordr). 2013; 35:1975–1982. [PubMed: 22986583]

3. Apple FS, Rhodes M. Enzymatic estimation of skeletal muscle damage by analysis of changes in serum creatine kinase. Journal of applied physiology. 1988; 65:2598–2600. [PubMed: 3215860]
4. Hagisawa S, Ferguson-Pell MW, Palmieri VR, Cochran GV. Pressure sores: A biochemical test for early detection of tissue damage. Arch Phys Med Rehabil. 1988; 69:668–671. [PubMed: 3421821]
5. Volfinger L, Lassourd V, Michaux JM, Braun JP, Toutain PL. Kinetic evaluation of muscle damage during exercise by calculation of amount of creatine kinase released. Am J Physiol. 1994; 266:R434–441. [PubMed: 8141400]
6. Wallimann T, Wyss M, Brdiczka D, Nicolay K, Eppenberger HM. Intracellular compartmentation, structure and function of creatine kinase isoenzymes in tissues with high and fluctuating energy demands: The 'phosphocreatine circuit' for cellular energy homeostasis. Biochem J. 1992; 281(Pt 1):21–40. [PubMed: 1731757]
7. Schlattner U, Tokarska-Schlattner M, Wallimann T. Mitochondrial creatine kinase in human health and disease. Biochim Biophys Acta. 2006; 1762:164–180. [PubMed: 16236486]
8. Bessman SP, Geiger PJ. Transport of energy in muscle: The phosphorylcreatine shuttle. Science. 1981; 211:448–452. [PubMed: 6450446]
9. Guimaraes-Ferreira L. Role of the phosphocreatine system on energetic homeostasis in skeletal and cardiac muscles. Einstein (Sao Paulo). 2014; 12:126–131. [PubMed: 24728259]
10. Gasper MC, Gilchrist JM. Creatine kinase: A review of its use in the diagnosis of muscle disease. Med Health R I. 2005; 88:398, 400–394. [PubMed: 16363394]
11. Silvestri NJ, Wolfe GI. Asymptomatic/pauci-symptomatic creatine kinase elevations (hyperckemia). Muscle Nerve. 2013; 47:805–815. [PubMed: 23625835]
12. Kodatsch I, Finsterer J, Stollberger C. Serum creatine kinase elevation in a medical department. Acta Med Austriaca. 2001; 28:11–15. [PubMed: 11253625]
13. Clarkson PM, Eichner ER. Exertional rhabdomyolysis: Does elevated blood creatine kinase foretell renal failure? Curr Sports Med Rep. 2006; 5:57–60. [PubMed: 16529674]
14. Ferrari M, Guasti L, Maresca A, Mirabile M, Contini S, Grandi AM, Marino F, Cosentino M. Association between statin-induced creatine kinase elevation and genetic polymorphisms in slco1b1, abcb1 and abcg2. Eur J Clin Pharmacol. 2014; 70:539–547. [PubMed: 24595600]
15. Fukami M, Maeda N, Fukushige J, Kogure Y, Shimada Y, Ogawa T, Tsujita Y. Effects of hmg-coa reductase inhibitors on skeletal muscles of rabbits. Res Exp Med (Berl). 1993; 193:263–273. [PubMed: 8278673]
16. Israeli A, Raveh D, Arnon R, Eisenberg S, Stein Y. Lovastatin and elevated creatine kinase: Results of rechallenge. Lancet. 1989; 1:725. [PubMed: 2564533]
17. Thompson PD, Nugent AM, Herbert PN. Increases in creatine kinase after exercise in patients treated with hmg co-a reductase inhibitors. JAMA. 1990; 264:2992. [PubMed: 2243421]
18. Hekimsoy Z, Oktem IK. Serum creatine kinase levels in overt and subclinical hypothyroidism. Endocrine research. 2005; 31:171–175. [PubMed: 16392619]
19. Sudarsanan S, Omar AS, Pattath RA, Al Mulla A. Acute kidney injury associated with rhabdomyolysis after coronary artery bypass graft: A case report and review of the literatures. BMC Res Notes. 2014; 7:152. [PubMed: 24636137]
20. Barbano B, Sardo L, Gasperini ML, Gigante A, Liberatori M, Giraldi GD, Di Mario F, Dorelli B, Amoroso A, Cianci R. Drugs and rhabdomyolysis: From liver to kidney. Curr Vasc Pharmacol. 2015
21. Chiong M, Wang ZV, Pedrozo Z, Cao DJ, Troncoso R, Ibacache M, Criollo A, Nemchenko A, Hill JA, Lavandero S. Cardiomyocyte death: Mechanisms and translational implications. Cell death & disease. 2011; 2:e244. [PubMed: 22190003]
22. Kim NH, Kang PM. Apoptosis in cardiovascular diseases: Mechanism and clinical implications. Korean Circ J. 2010; 40:299–305. [PubMed: 20664736]
23. Takemura G, Fujiwara H. Role of apoptosis in remodeling after myocardial infarction. Pharmacology & therapeutics. 2004; 104:1–16. [PubMed: 15500905]
24. Takemura G, Kanoh M, Minatoguchi S, Fujiwara H. Cardiomyocyte apoptosis in the failing heart--a critical review from definition and classification of cell death. Int J Cardiol. 2013; 167:2373–2386. [PubMed: 23498286]

25. van Empel VP, Bertrand AT, Hofstra L, Crijns HJ, Doevendans PA, De Windt LJ. Myocyte apoptosis in heart failure. Cardiovasc Res. 2005; 67:21–29. [PubMed: 15896727]
26. Wang X, Parrish AR. Loss of alpha(e)-catenin promotes fas mediated apoptosis in tubular epithelial cells. Apoptosis. 2015; 20:921–929. [PubMed: 25894537]
27. Kim S, Bi X, Czarny-Ratajczak M, Dai J, Welsh DA, Myers L, Welsch MA, Cherry KE, Arnold J, Poon LW, Jazwinski SM. Telomere maintenance genes sirt1 and xrcc6 impact age-related decline in telomere length but only sirt1 is associated with human longevity. Biogerontology. 2012; 13:119–131. [PubMed: 21972126]
28. D'Mello NP, Childress AM, Franklin DS, Kale SP, Pinswasdi C, Jazwinski SM. Cloning and characterization of lag1, a longevity-assurance gene in yeast. J Biol Chem. 1994; 269:15451–15459. [PubMed: 8195187]
29. Tepper CG, Jayadev S, Liu B, Bielawska A, Wolff R, Yonehara S, Hannun YA, Seldin MF. Role for ceramide as an endogenous mediator of fas-induced cytotoxicity. Proc Natl Acad Sci U S A. 1995; 92:8443–8447. [PubMed: 7545303]
30. Herget T, Esdar C, Oehrlein SA, Heinrich M, Schutze S, Maelicke A, van Echten-Deckert G. Production of ceramides causes apoptosis during early neural differentiation in vitro. J Biol Chem. 2000; 275:30344–30354. [PubMed: 10862608]
31. Bose R, Verheij M, Haimovitz-Friedman A, Scotto K, Fuks Z, Kolesnick R. Ceramide synthase mediates daunorubicin-induced apoptosis: An alternative mechanism for generating death signals. Cell. 1995; 82:405–414. [PubMed: 7634330]
32. Jazwinski SM, Kim S, Dai J, Li L, Bi X, Jiang JC, Arnold J, Batzer MA, Walker JA, Welsh DA, Lefante CM, Volaufova J, Myers L, Su LJ, Hausman DB, Miceli MV, Ravussin E, Poon LW, Cherry KE, Welsch MA, Georgia Centenarian S. the Louisiana Healthy Aging S. Hras1 and lass1 with apoe are associated with human longevity and healthy aging. Aging Cell. 2010; 9:698–708. [PubMed: 20569235]
33. Barrett JC. Haploview: Visualization and analysis of snp genotype data. Cold Spring Harb Protoc. 2009; 2009 pdb ip71.
34. Barrett JC, Fry B, Maller J, Daly MJ. Haploview: Analysis and visualization of ld and haplotype maps. Bioinformatics. 2005; 21:263–265. [PubMed: 15297300]
35. Dipietro L, Caspersen CJ, Ostfeld AM, Nadel ER. A survey for assessing physical activity among older adults. Med Sci Sports Exerc. 1993; 25:628–642. [PubMed: 8492692]
36. Fillee C, Vranken G, Othmane M, Philippe M, Allaeys JM, Courbe A, Ruelle JL, Peeters R. Results of the recalibration of creatinine measurement with the modular beckman coulter jaffe creatinine method. Clin Chem Lab Med. 2011; 49:1987–1999. [PubMed: 21801031]
37. Levey AS, Bosch JP, Lewis JB, Greene T, Rogers N, Roth D. A more accurate method to estimate glomerular filtration rate from serum creatinine: A new prediction equation. Modification of diet in renal disease study group. Ann Intern Med. 1999; 130:461–470. [PubMed: 10075613]
38. Levey AS, Stevens LA, Schmid CH, Zhang YL, Castro AF 3rd, Feldman HI, Kusek JW, Eggers P, Van Lente F, Greene T, Coresh J. A new equation to estimate glomerular filtration rate. Ann Intern Med. 2009; 150:604–612. [PubMed: 19414839]
39. R_Core_Team. R: A language and environment for statistical computing. Vienna, Austria: R Foundation for Statistical Computing; 2014.
40. Faul F, Erdfelder E, Buchner A, Lang AG. Statistical power analyses using g*power 3. 1: Tests for correlation and regression analyses. Behavior research methods. 2009; 41:1149–1160. [PubMed: 19897823]
41. Kim S, Jazwinski SM. Quantitative measures of healthy aging and biological age. Healthy Aging Res. 2015; 4
42. Schneider CM, Dennehy CA, Rodearmel SJ, Hayward JR. Effects of physical activity on creatine phosphokinase and the isoenzyme creatine kinase-mb. Ann Emerg Med. 1995; 25:520–524. [PubMed: 7710160]
43. Ernst J, Kheradpour P, Mikkelsen TS, Shoresh N, Ward LD, Epstein CB, Zhang X, Wang L, Issner R, Coyne M, Ku M, Durham T, Kellis M, Bernstein BE. Mapping and analysis of chromatin state dynamics in nine human cell types. Nature. 2011; 473:43–49. [PubMed: 21441907]

44. Ward LD, Kellis M. Haploreg: A resource for exploring chromatin states, conservation, and regulatory motif alterations within sets of genetically linked variants. Nucleic Acids Res. 2012; 40:D930–934. [PubMed: 22064851]
45. Boulton SJ, Jackson SP. Components of the ku-dependent non-homologous end-joining pathway are involved in telomeric length maintenance and telomeric silencing. EMBO J. 1998; 17:1819–1828. [PubMed: 9501103]
46. Reddel RR, Bryan TM, Colgin LM, Perrem KT, Yeager TR. Alternative lengthening of telomeres in human cells. Radiat Res. 2001; 155:194–200. [PubMed: 11121234]
47. Riha K, Heacock ML, Shippen DE. The role of the nonhomologous end-joining DNA double-strand break repair pathway in telomere biology. Annu Rev Genet. 2006; 40:237–277. [PubMed: 16822175]
48. Celli GB, Denchi EL, de Lange T. Ku70 stimulates fusion of dysfunctional telomeres yet protects chromosome ends from homologous recombination. Nat Cell Biol. 2006; 8:885–890. [PubMed: 16845382]
49. Hada M, Kwok RP. Regulation of ku70-bax complex in cells. J Cell Death. 2014; 7:11–13. [PubMed: 25278782]
50. Sawada M, Sun W, Hayes P, Leskov K, Boothman DA, Matsuyama S. Ku70 suppresses the apoptotic translocation of bax to mitochondria. Nat Cell Biol. 2003; 5:320–329. [PubMed: 12652308]
51. Meng J, Zhang F, Zhang XT, Zhang T, Li YH, Fan L, Sun Y, Zhang HL, Mei QB. Ku70 is essential for histone deacetylase inhibitor trichostatin a-induced apoptosis. Molecular medicine reports. 2015; 12:581–586. [PubMed: 25695595]
52. Subramanian C, Jarzembowski JA, Opipari AW Jr, Castle VP, Kwok RP. Hdac6 deacetylates ku70 and regulates ku70-bax binding in neuroblastoma. Neoplasia. 2011; 13:726–734. [PubMed: 21847364]
53. Seluanov A, Danek J, Hause N, Gorbunova V. Changes in the level and distribution of ku proteins during cellular senescence. DNA Repair (Amst). 2007; 6:1740–1748. [PubMed: 17686666]
54. Turpin SM, Lancaster GI, Darby I, Febbraio MA, Watt MJ. Apoptosis in skeletal muscle myotubes is induced by ceramides and is positively related to insulin resistance. Am J Physiol Endocrinol Metab. 2006; 291:E1341–1350. [PubMed: 16849630]
55. Pilane CM, LaBelle EF. No induced apoptosis of vascular smooth muscle cells accompanied by ceramide increase. J Cell Physiol. 2004; 199:310–315. [PubMed: 15040013]
56. von Haefen C, Wieder T, Gillissen B, Starck L, Graupner V, Dorken B, Daniel PT. Ceramide induces mitochondrial activation and apoptosis via a bax-dependent pathway in human carcinoma cells. Oncogene. 2002; 21:4009–4019. [PubMed: 12037683]
57. Senkal CE, Ponnusamy S, Rossi MJ, Bialewski J, Sinha D, Jiang JC, Jazwinski SM, Hannun YA, Ogretmen B. Role of human longevity assurance gene 1 and c18-ceramide in chemotherapy-induced cell death in human head and neck squamous cell carcinomas. Mol Cancer Ther. 2007; 6:712–722. [PubMed: 17308067]
58. Park SY, Lee JH, Kim HY, Yoon KH, Park SK, Chang MS. Differential expression of apoptosis-related factors induces the age-related apoptosis of the gracilis muscle in humans. Int J Mol Med. 2014; 33:1110–1116. [PubMed: 24584667]
59. Gouspillou G, Sgarioto N, Kapchinsky S, Purves-Smith F, Norris B, Pion CH, Barbat-Artigas S, Lemieux F, Taivassalo T, Morais JA, Aubertin-Leheudre M, Hepple RT. Increased sensitivity to mitochondrial permeability transition and myonuclear translocation of endonuclease g in atrophied muscle of physically active older humans. Faseb j. 2014; 28:1621–1633. [PubMed: 24371120]
60. Fulle S, Sancilio S, Mancinelli R, Gatta V, Di Pietro R. Dual role of the caspase enzymes in satellite cells from aged and young subjects. Cell death & disease. 2013; 4:e955. [PubMed: 24336075]
61. Jiang X, Wang X. Cytochrome c promotes caspase-9 activation by inducing nucleotide binding to apaf-1. J Biol Chem. 2000; 275:31199–31203. [PubMed: 10940292]
62. Marzetti E, Lees HA, Manini TM, Buford TW, Aranda JM Jr, Calvani R, Capuani G, Marsiske M, Lott DJ, Vandenborne K, Bernabei R, Pahor M, Leeuwenburgh C, Wohlgemuth SE. Skeletal

muscle apoptotic signaling predicts thigh muscle volume and gait speed in community-dwelling older persons: An exploratory study. PLoS One. 2012; 7:e32829. [PubMed: 22389725]

63. Hazra NC, Dregan A, Jackson S, Gulliford MC. Differences in health at age 100 according to sex: Population-based cohort study of centenarians using electronic health records. J Am Geriatr Soc. 2015; 63:1331–1337. [PubMed: 26096699]
64. Stupka N, Lowther S, Chorneyko K, Bourgeois JM, Hogben C, Tarnopolsky MA. Gender differences in muscle inflammation after eccentric exercise. Journal of applied physiology. 2000; 89:2325–2332. [PubMed: 11090586]
65. Khoury MJ, Evans JP. A public health perspective on a national precision medicine cohort: Balancing long-term knowledge generation with early health benefit. Jama. 2015; 313:2117–2118. [PubMed: 26034952]
66. Hoenig JM, Heisey DM. The abuse of power. The American Statistician. 2001; 55:19–24.
67. Goodman SN, Berlin JA. The use of predicted confidence intervals when planning experiments and the misuse of power when interpreting results. Ann Intern Med. 1994; 121:200–206. [PubMed: 8017747]

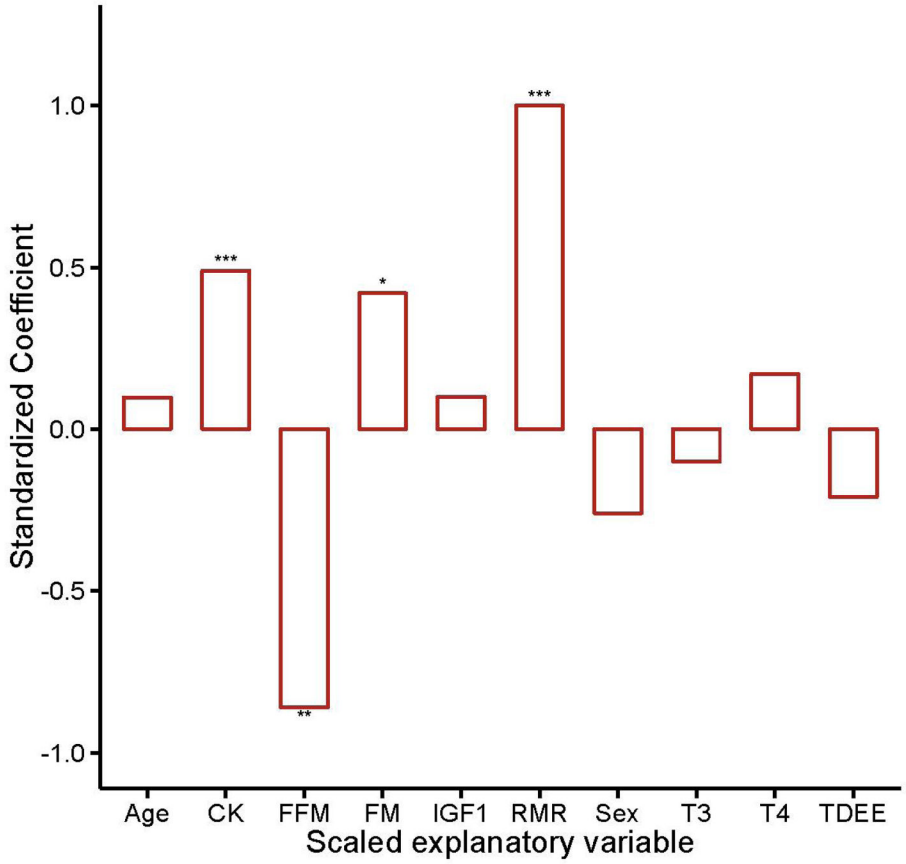

Fig.1.

Standardized coefficients from multiple linear regression in which the dependent variable is FI_{34} and the explanatory variables are as indicated on the x axis. CK = circulating creatine kinase, FFM = fat-free mass, FM = fat mass, IGF1 = insulin-like growth factor 1, RMR = resting metabolic rate, T3 = tri-iodothyronine, T4 = thyroxine, TDEE = total daily energy expenditure. The subjects were 67 nonagenarians. Adjusted $R^2 = 0.63$, F-test p value < 0.0001; * 0.01 < P value < 0.05, ** 0.001 < p value < 0.01, *** p value < 0.001

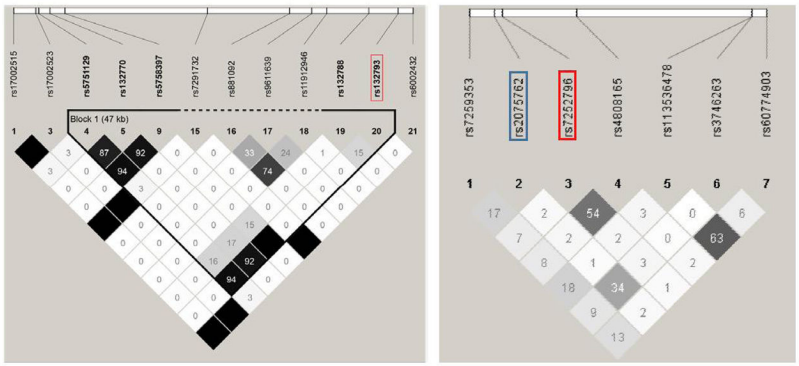

Fig. 2.

LD structure involving SNPs around rs132793 in *XRCC6* (left) and rs2075762 and rs7252796 in *LASS1* (right) with the Haploview r^2 Color Scheme in which white blocks represent $r^2 = 0$; shades of grey, $0 < r2 < 1$; black, $r^2 = 1$.

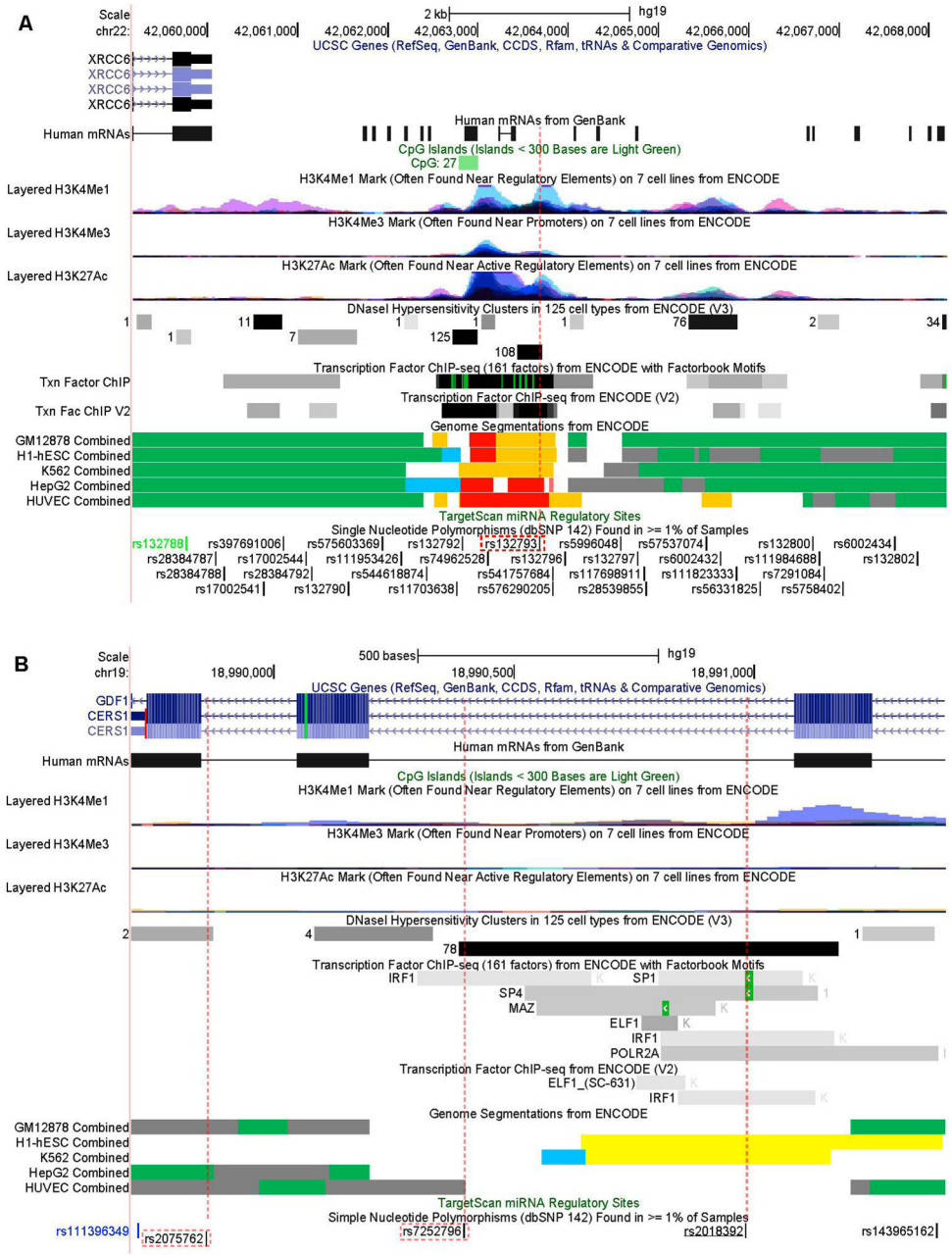

Fig. 3.

Genomic features around rs132793 near *XRCC6* (A) and rs2075762 and rs7252796 in *LASS1* (B) (from the UCSC Genome Browser). SNPs analyzed in this study are enclosed in red-dotted rectangles. SNP rs2018392 (underlined in B) is in high LD with rs7252796. SNP IDs in black are in introns, green in coding (synonymous), and blue in untranslated regions. The CpG Islands track shows a segment with the GC content = 50%, the length > 200 bp and the ratio observed to expected CpG > 0.6. The number of CG dinucleotides are shown in front of the segment. Colors in histone modification tracks represent results from different cell lines, and peak levels show enrichment levels of corresponding histone marks. DNase I

Hypersensitivity Clusters indicate hypersensitive sites to DNase I with the darkness proportional to the sensitivity. The number to the left of each box shows the number of cell lines where the region was hypersensitive. The Transcription Factor ChIP-seq tracks show transcription factor binding sites from ChIP-seq experiments. The darkness is proportional to the signal strength, and the green highlights indicate the highest scoring-site motifs. The Genome Segmentations represent chromatin segments corresponding to different functional states: Green segments represent predicted transcribed regions; blue segments, CTCF enriched segments; yellow, predicted weak enhancers or open chromatin cis regulatory elements; orange, predicted enhancers; grey, predicted repressed or low activity regions.

Table 1

Basic characteristics of the study sample

Variable	All (n=67)	Male (n=30)	Female (n=37)
Age (years)	92 ± 2	92 ± 2	92 ± 2
FI_{34}[1]	0.208 ± 0.073	0.182 ± 0.071	0.230 ± 0.067
EESI (kcal/d)	3677.7 ± 2921.3	3731.5 ± 3038.3	3632.8 ± 2862.8
RMR (kcal/d)[2]	1142.3 ± 183.5	1281.8 ± 147.3	1029.2 ± 122.0
FM (kg)	20.4 ± 6.6	19.8 ± 4.9	20.9 ± 7.6
FFM (kg)[3]	44.0 ± 9.5	52.1 ± 5.1	37.4 ± 5.3
CK (IU/L)[4]	72.0 ± 50.5	80.5 ± 61.5	60.0 ± 35.0
CKt[5]	0.12 ± 0.030	0.12 ± 0.034	0.13 ± 0.026
Cardiac[6]	0 ± 2	0 ± 1	0 ± 2
eGFR (CKD-EPI)[7]	51.9 ± 15.0	48.9 ± 15.0	54.2 ± 14.7
BSA[8]	1.7 ± 0.2	1.8 ± 0.1	1.6 ± 0.2

Numbers are means ± standard deviations (median ± interquartile range for CK and Cardiac). FI_{34} = a frailty index based on 34 health variables, EESI = Energy Expenditure Summary Index of the Yale Physical Activity Survey, RMR = resting metabolic rate, FM = fat mass, FFM = fat-free mass, CK = creatine kinase, CKt = transformed CK ($CK^{-0.5}$), eGFR = estimated glomerular filtration rate in mL/min/1.73 m^2 by the chronic kidney disease epidemiology collaboration (CKD-EPI) equation, BSA = body surface area calculated using the Mosteller formula (m^2 = square root of ([height(cm) x Weight(kg)]/ 3600);

[1] $p = 0.0029$ between sexes by a Wilcoxon rank sum test ($p = 0.0066$ by t test);

[2] $p < 0.001$ between sexes by a Wilcoxon rank sum test ($p < 0.001$ by t test);

[3] $p < 0.001$ between sexes by a Wilcoxon rank sum test ($p < 0.001$ by t test);

[4–7] $p > 0.05$ between sexes.

Table 2

Association of heart problems and eGFR with CKt levels in male nonagenarians by two-way ANOVA

Variable	Df	Sum Sq	Mean Sq	F value	*P*
Cardiac	1	55300	55300	7.932	0.00091
eGFR	1	44801	44801	6.426	0.018
Cardiac x eGFR	1	12384	12384	1.7762	0.194174
Residuals	26	181274	6972		

Cardiac denotes the presence or absence of one or more heart-related problems in medical history (angina, congestive heart failure, heart attack, heart murmur, and other unspecified heart problem). eGFR denotes eGFR values lower than 60 or ≥60 by the CKD-EPI equation.

Table 3

Comparison of nested linear regressions with CKt as the dependent variable

	Male nonagenarians (n=30)			
	Model 1		Model 2	
Variable	**b**	***p***	**b**	***p***
Cardiac	−0.015	1.1e-3	−0.014	1.2e-4
eGFR	1.0e-3	1.4e-3	1.1e-3	2.7e-4
EESI	-	-	3.4e-6	0.019
R^2_a	0.52 (0.56)		0.60 (0.64)	
P_F	1.7e-5		5.4e-6	

eGFR = estimated glomerular filtration rate by the CKD-EPI equation, Cardiac = the number of heart-related problems in individual medical histories; EESI = Energy Expenditure Summary Index of the Yale Physical Activity Survey (kcal/wk); CKt = transformed CK; R^2_a = adjusted R^2 (unadjusted); P_F = *p* value from the F-test.

Table 4

Association of SNPs linked to *XRCC6* and *LASS1* with CKt in nonagenarian males

Variable	rs132793			rs2075762			rs7252796		
	b	**se.b**	***p***	**b**	**se.b**	***p***	**b**	**se.b**	***p***
Cardiac	−9.5e-3	2.5e-3	8.0e-4	−1.3e-2	2.7e-3	5.5e-5	−1.5e-2	2.7e-3	9.1e-6
eGFR	1.1e-3	2.0e-4	5.9e-6	8.6e-4	2.5e-4	8.6e-4	1.3e-3	2.4e-4	1.6e-5
EESI	3.9e-6	1.0e-6	7.0e-4	3.0e-6	1.2e-6	1.8e-2	2.9e-6	1.2e-6	2.4e-2
SNP	2.4e-2	5.2e-3	8.4e-5	2.6e-2	8.6e-3	6.1e-3	−2.8e-2	9.6e-3	6.9e-3
Model	df=25, R^2=0.78, P_F=1.1e-8			df=25, R^2=0.69, P_F=5.8e-7			df=24, R^2=0.71, P_F=5.8e-7		

CKt = transformed creatine kinase; Cardiac = the number of heart-related problems in individual medical histories; EESI = Energy Expenditure Summary Index of the Yale Physical Activity Survey; eGFR = eGFR by the CKD-EPI equation; SNP = additive genotype model; Model = model statistics for each regression model; b = regression coefficient; se.b = standard error of b; df = degrees of freedom; R^2 = adjusted R^2; P_F = *p* value from the F-test.

Table 5

Association of combinations of SNPs with CKt in nonagenarian males

	Model 1		Model 2		Model 3		Model 4	
Variable	**b**	***p***	**b**	***p***	**b**	***p***	**b**	***p***
Cardiac	−9.8e-3	3.8e-4	−1.1e-2	9.8e-5	−1.4e-2	3.7e-6	−1.1e-2	3.8e-5
eGFR	1.0e-3	3.0e-5	1.2e-3	8.6e-7	1.1e-3	5.0e-5	1.1e-4	3.6e-6
EESI	3.6e-6	1.1e-3	3.4e-6	1.4e-3	2.6e-6	0.023	3.1e-6	2.1e-3
rs132793	2.0e-2	9.4e-4	2.0e-2	5.0e-4	-	-	1.6e-2	3.6e-3
rs2075762	1.4e-2	0.069	-	-	2.2e-2	7.1e-3	1.4e-2	0.050
rs7252796	-	-	−2.0e-2	0.018	−2.6e-2	5.0e-3	−2.0e-2	0.012
Model	df=23, R^2 = 0.80, P_F = 1.2e-8		df=23, R^2 = 0.82, P_F = 6.6e-9		df=23, R^2 = 0.78, P_F = 7.4e-8		df=22, R^2 = 0.84, P_F = 5.4e-9	
P_{anova}	0.069[a]		0.018[a]		7.1e-3[b]		9.0e-3[a]	

CKt = transformed creatine kinase; Cardiac = the number of heart-related problems in individual medical histories; EESI = Energy Expenditure Summary Index of the Yale Physical Activity Survey; eGFR = eGFR by the CKD-EPI equation; SNP = additive genotype model; Model = model statistics for each regression model; b = regression coefficient; se.b = standard error of b; df = degrees of freedom; R^2 = adjusted R^2; P_F = *p* value from the F-test; P_{anova} is the *p* value from an ANOVA test between the model specified and the model with only rs132793 (a) or with only rs2075762 (b) shown in Table 4.